Modeling Earth Systems and Environment (2024) 10:4361–4373
https://doi.org/10.1007/s40808-024-02023-1

ORIGINAL ARTICLE

Modeling geothermal energy potential in the Ruwan-Zafi hot spring region of northeastern Nigeria using high-resolution aeromagnetic data

Ema Abraham[1] · **Princewill Okechukwu**[1,2]

Received: 27 March 2024 / Accepted: 13 April 2024 / Published online: 9 May 2024

Abstract

Renewable energy has become a viable solution to tackle energy challenges in Africa, and Nigeria is actively exploring various options to enhance its energy supply. Geothermal energy has attracted significant attention, especially following the discovery of multiple geothermal sites across the country. This study focuses on the Ruwan-Zafi Hot Spring (RZHS) region with the aim of investigating its suitability for geothermal energy exploration and exploitation. Spectral analysis of aeromagnetic data was used to model the depths to the top (DTT) and centroid of subsurface magnetic source. Through these computations, the depth to the bottom of magnetic source (assumed Curie Point Depth, CPD) was derived for the region. Results show DTT values ranging between 0.89 and 1.08 km, and CPDs ranging between 9.96 and 14.92 km. In addition, estimated heat flow values ranged between 73.62 and 128.39 mWm^{-2}. The shallow CPD and high heat flow values within the RZHS area is largely due to magmatic intrusions at depth and indicates the location's potential for geothermal energy resources. Results also suggest the possibility of steam production at shallow depths (<2 km). The identification of subsurface structures linked to geothermal reservoirs at the RZHS location offers valuable insights for guiding future geothermal exploration activities in the region and recommends further exploration and resource assessment.

Keywords Geothermal · Energy · Magnetic · Ruwan Zafi · Curie Point Depth

Introduction

Modeling the geothermal energy potential of a region involves assessing various geological, hydrological, and thermal factors to estimate the heat available for conversion into usable energy. Geothermal energy has emerged as a promising and sustainable alternative to traditional fossil fuel-based energy sources, offering the potential to address energy challenges in various regions, including Africa. Continuous access to energy is a critical concern for all nations in both the present and future. The growth of an economy depends heavily on the consistent availability of energy from sources that are affordable, readily accessible, and environmentally friendly. Without access to reliable energy sources, communities may struggle to meet their basic needs, leading to increased hardships and lower quality of life. Insufficient access to energy is linked to poverty, deprivation, and can lead to economic downturns (Grogan 2015; Sovacool and Dworkin 2015; Oyedepo 2012; Bazilian et al. 2011; Khandker et al. 2009; Kammen and Agusdinata 1997). The exploration and assessment of geothermal energy potential in the Ruwan-Zafi Hot Spring (RZHS) region of Northeastern Nigeria represent a critical endeavor within the broader context of sustainable energy development and environmental management. Despite indications of geothermal activity in the area, comprehensive studies integrating advanced modeling techniques with high-resolution geophysical data are lacking. The absence of such investigations hampers our ability to understand the geological structures, thermal dynamics, and environmental implications associated with geothermal resource exploitation. This study aims to address this gap by employing advanced geophysical modeling

✉ Ema Abraham
ema.abraham@funai.edu.ng

1 Department of Geology/Geophysics, Alex Ekwueme Federal University, Ndufu-Alike Ikwo, P.M.B. 1010, Abakaliki, Ebonyi State, Nigeria

2 Three and Three Consult Limited, Abuja, Nigeria

techniques on high-resolution aeromagnetic data to model the geothermal energy potential of the RZHS region. The integration of aeromagnetic data enables precise delineation of subsurface structures, facilitating accurate assessment of heat flow dynamics and resource distribution.

Although Nigeria is recognized for her abundant hydrocarbon resources, the country is increasingly prioritizing the diversification of her energy mix to meet escalating energy demands and tackle environmental challenges. Geothermal energy exploration and development have risen to strategic prominence in Nigeria's energy transition agenda, aimed at tapping into the country's untapped geothermal reservoirs. The RZHS region, nestled within the Chad Basin sedimentary basin, garners attention for its geological characteristics conducive to geothermal activity, evident through the presence of hot springs and elevated subsurface temperatures (Adepelumi and Olorunfemi 2019; Akintude et al. 2017). Quite a number of studies have been conducted to model renewable energy prospects of regions (Dar et al. 2024; Ijeh et al. 2023; Al-Ghriybah et al. 2023; Kassem et al. 2022; Rabeh and El Rahman 2022, Ishola et al. 2020; Selvarajoo et al. 2020; Yakubu et al. 2020; Akintude et al. 2017). For focus, we examine some of the geo-scientific aspects of these studies in Nigeria. Ishola et al. (2020) interpreted aeromagnetic data from Ewekoro, southeastern Nigeria to map subsurface geological structures. They observed lineaments majorly trending in NE–SW direction and interpreted these as faults or fractures in the region. Estimated depths of 0.02–0.75 km were also realized. Ijeh et al. (2023) assessed the geothermal resource potentials of Lower Benue Trough using high-resolution aeromagnetic and radiometric data. Observed curie depths, average geothermal gradient and the average heat flow of the Lower Benue Trough were 13.96742 km, 159.4072 mW/m^2 and 42.639 °C/km respectively. They concluded on the geothermal suitability of the study area for further investigations. Yakubu et al. (2020) estimated the Curie point depth (CPD), geothermal gradient and heat flow within Nigeria lower Benue trough using the spectral analysis method. The obtained Curie point depth values between 10.5 and 22.5 km, average geothermal gradient of 37.8 °C/km and heat flow averages of 96.22 mW/m^2. Consequently, they recommended further geothermal explorations in the region. Abraham et al. (2018) performed spectral analysis on aeromagnetic data to investigate geothermal energy potential in southeastern Nigeria. They determined the basal depths, also known as Curie Point Depth (CPD), in the region to range between 9.8 and 19.3 km. Ojoawo and Sedara (2016) discovered an approximate depth to basement rocks at Ikogosi region of southwestern Nigeria to range between 8 and 14 m from their horizontal profiling technique. The Wikki Warm Spring (WWS) area in Bauchi State, northeastern Nigeria, have also been subjected to geophysical analysis. Initial study (Obande et al. 2014) indicate relatively shallow Curie Point Depth (CPD) values for the WWS region. With estimated CPD values ranging from 8 to 11 km, these researchers suggested further exploration of the area for geothermal potential. Eeltta and Udensi (2012) and Emetere and Akpan (2022) have conducted some geo-scientific investigations on the southeast of Nigeria. They adopted the spectral analysis, well evaluations and remote sensing approaches to pinpoint locations for further investigations. At the northern region of the country, spectral analysis of aeromagnetic anomalies was also undertaken by Anakwuba et al. (2016). Although their results of 21.45 km and 31.52 km were comparatively deeper compared to the other parts of the country, suggesting non-viability for geothermal considerations, they however affirmed the suitability of the method to provide adequate geothermal depths information at a location. Onyejiuwaka and Iduma (2020) attempted to investigate the RZHS region using aeromagnetic data and reported a depth range between 8.4 and 17.16 km for the location. However, we contend that their deductions may be erroneous due to the lack of proper implementation of basic concepts for CPD investigations. One of the flaws identified is the use of insufficient data and non-overlapping window sizes, which may have only provided information for half of its size, thus not reaching the acclaimed RZHS location depths, as given in their study. However, CPD values were provided to cover the entire region. The present study covers the entire region of the warm spring location with sufficient magnetic data and aims to properly investigate the geothermal energy potentials, model the isotherm depths, and estimate heat flow at the RZHS region. Through the integration of aeromagnetic data with computational modeling approaches, this study seeks to elucidate the spatial distribution of geothermal resources, assess heat flow dynamics, and evaluate the environmental implications of geothermal energy extraction in the RZHS region. The objective is to pinpoint locations with promising geothermal resources, determine their depths, and estimate heat flow based on the results. This analysis will provided valuable insights into the geothermal resource suitability of the region, shedding light on the potential for steam production at shallow depths and identifying anomalous geothermal conditions within the subsurface. The results of this study have substantial implications for the future development of geothermal energy in Nigeria, contributing to the broader discourse on sustainable energy development and environmental modeling.

The study area

The study are locates at the northeastern region of Nigeria (Fig. 1). RZHS is on Latitude 9.60°N and Longitude 11.78°E at Bachama, Lamurde Local Government Area of Adamawa State. During rainy seasons, a part of the spring is cool while the other part is boiling hot from the same source. The topography (physical features of the land) of the region shows high elevations at the NW, NE, Southern and most part of the Central region (Fig. 2). All the high elevations slopes down towards the central region of the Benue River, traversing the study area. RZHS, with an average temperature of 54 °C is sited within a huge tectonic structure – Lamurde anticline, north of the Benue Trough. Topographic features such as mountains, valleys, and fault lines can be indicative of tectonic activity. We believe that the existence of the RZHS in the region could have been connected with the tectonic activities that ensued at the region.

The topography of a region can be influenced by underlying geological structures such as rock types, faults, and folds. This is evident from the geological map (Fig. 3) of the area. In the Upper Benue Trough, the basement is covered by the Aptian-Albian Bima sandstone, which is the oldest, thickest, and most widely exposed formation in the trough (Haruna et al. 2012).

Guiraud's (1990) sedimentological analysis revealed that the Bima sandstone can be categorized into three distinct silicaclastic members: the Lower, Middle, and Upper Bima Members. These members are characterized by the presence of basaltic and rhyolitic clasts, as well as rhyolitic to basaltic volcanic lenses, indicating concurrent volcanic activity (Guiraud 1990; Guiraud and Maurin 1992). The Bima sandstone is succeeded by transitional interbeds of shale, siltstone, and calcareous mudstone of the Yolde Formation (Cenomanian-Turonian), which transition into thick limestone beds and shale of the Gongola Formation in the Gongola sub-basin, and its lateral equivalents: the Dukul Formation (comprising mainly gray shales and thin silty beds), and the Jessu and Numanha Formations in the Yola Sub-basin. These sequences are followed by poorly to moderately sorted sandstone of the Gombe Formation (Campanian-Maastrichtian) in the Gongola sub-basin and the Lamja sandstone in the Yola Arm. The succession is topped by sandstone of the Keri-Keri Formation (located west of Gombe town) in the Gongola Arm.

The Upper Benue Trough (Fig. 3) is characterized by a significant number of NE – SW trending mylonitic shear

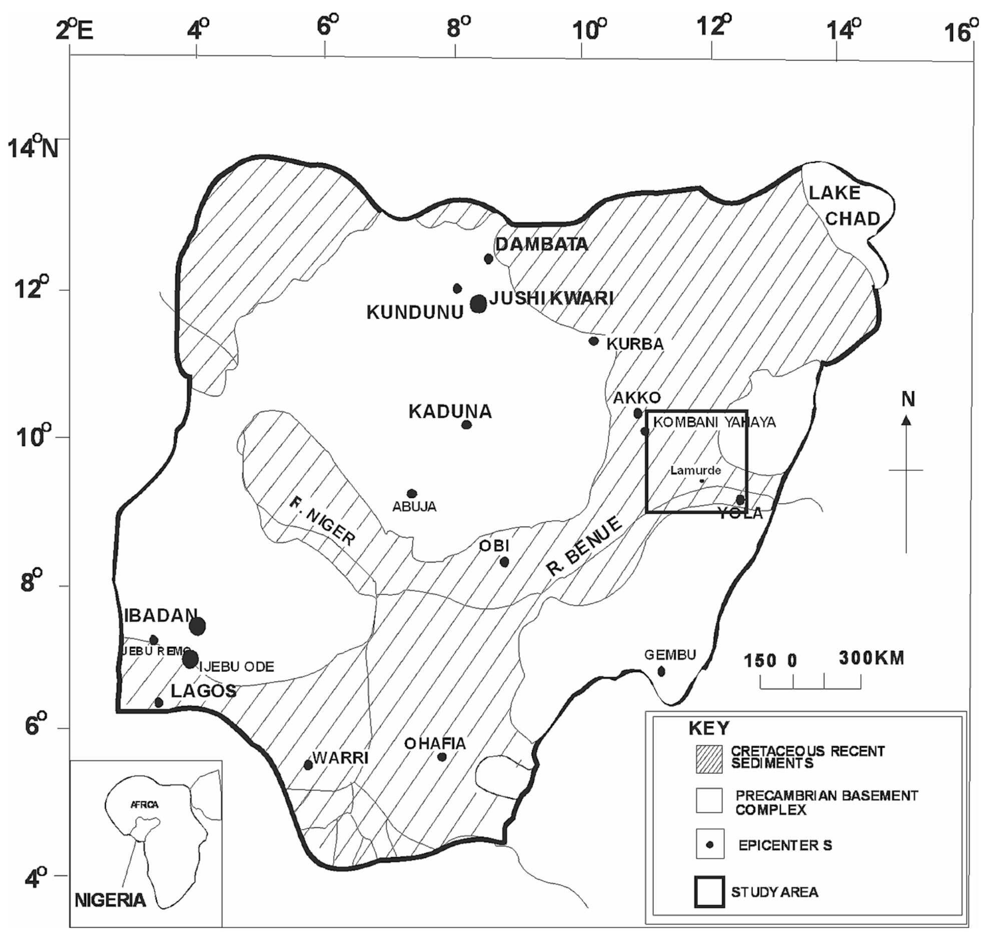

Fig. 1 Map of Nigeria showing the study area. The general geology of the country is also shown

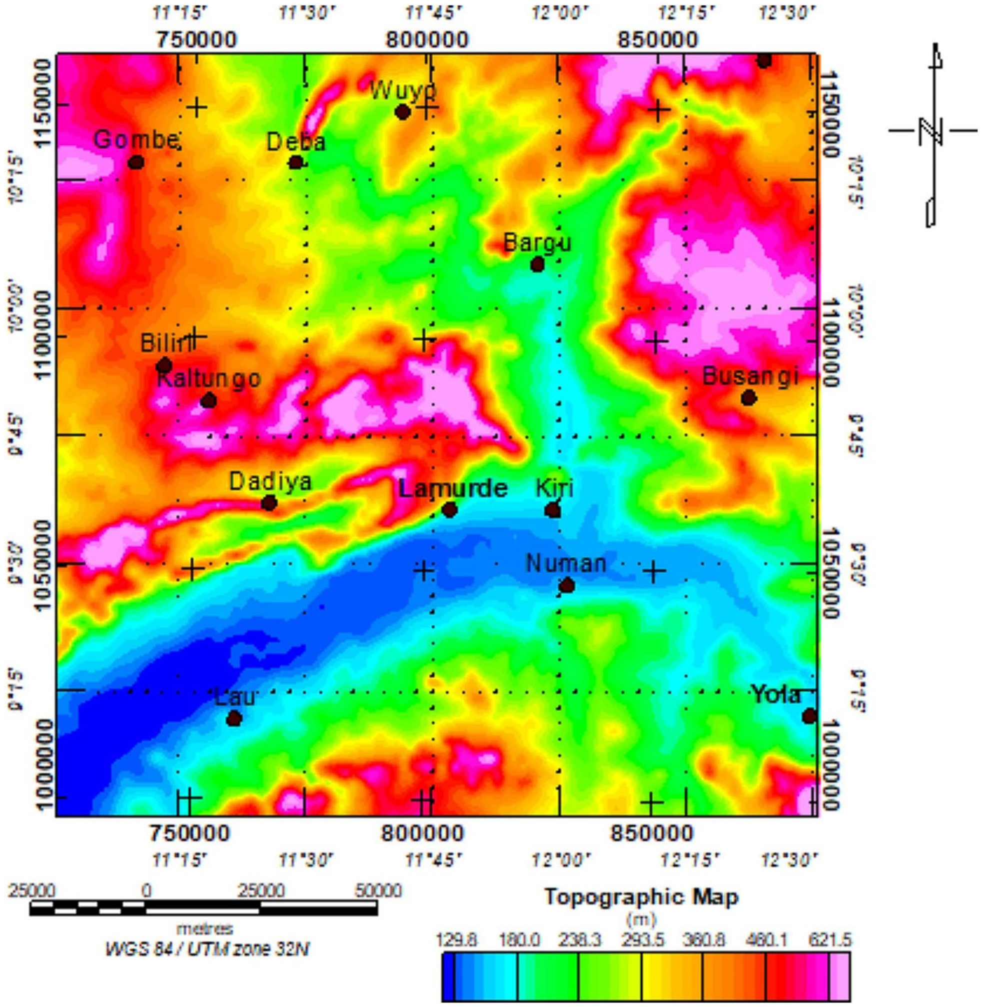

Fig. 2 Topographic map of the study region

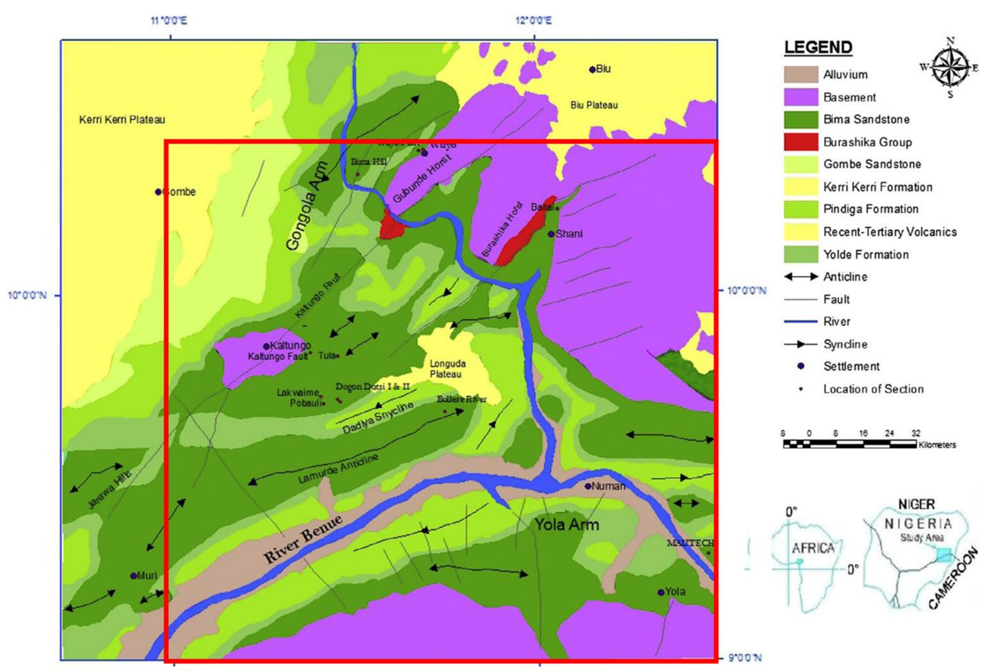

Fig. 3 Geologic map of the Upper Benue Trough showing the study area. (Modified after Benkhelil (1986)

zones, which were formed during the late Pan-African phase and later reactivated as sinistral strike-slip faults during the Cretaceous period (Benkhelil and Robineau 1983; Benkhelil 1986; Maurin et al. 1985). Notably, three primary fracture zones trending northeast have been identified: the Gombe fault, the Kwol-Kaltungo lineament, which spans approximately 150 km, and the Burashika fault. These major fractures intersect the Cretaceous deposits and impact the underlying basement. The major fractures in this area exhibit tectonic deformation through cataclastic and brecciated bands, which are approximately 300 m to 1 km wide in the basement, and crushed zones about 100 m wide in the sedimentary cover. This deformation overlays the Pan-African mylonitic shear zones and creates post-depositional fracture/fault zones (Haruna et al. 2012). The boundary of the Upper Benue Trough in the area between the N – E trending southern domain (Muri-Lamurde branch) and Yola arm is delineated by three northeast trending fault-bounded Early Cretaceous sub-basins: the Nahantsi, Kurkude, and Shani sub-basins. Adjacent to these sub-basins are two NE – SW trending uplifted basement blocks: the Wuyo-Guburunde Horst and the Burashika Horst. A large-scale NE – SW trending Lamurde anticline and Dadiya syncline in the Upper Benue Trough were formed by a general N – E compression that impacted the Northern part of the Benue Trough at the conclusion of the Cretaceous period (Benkhelil 1982, 1986).

Methodology

One method for modeling the thermal structure of the Earth's crust involves the estimation of the Curie Point Depth (CPD) using aeromagnetic data (Dolmaz et al. 2005). Numerous studies have established correlations between Curie temperature depths and average crustal temperatures, leading to meaningful insights into lithospheric thermal conditions in various regions worldwide (Ross et al. 2006). The techniques for determining the depth range of magnetic sources can be classified into those that analyze the shape of isolated magnetic anomalies (e.g. Bhattacharyya and Leu 1975) and those that consider the statistical characteristics of magnetic anomaly patterns (e.g. Spector and Grant 1970). By converting the spatial data into the frequency domain, both techniques demonstrate the relationship between the spectra of magnetic anomalies and the depth of magnetic sources (Tanaka et al. 1999; Obande et al. 2014). CPD investigations were determined for some parts of Japan (Okubo et al. 1985), India (Rajaram et al. 2009; Bansal et al. 2013), USA (Blakely 1988; Mayhew 1985), Greece (Stampolidis and Tsokas 2002; Tsokas et al. 1998), Bulgaria (Trifonova et al. 2006, 2009), Turkey (Dolmaz et al. 2005; Maden 2009), Mexico (Manea and Manea 2011), Portugal (Okubo et al. 2003) and Nigeria (Obande et al. 2014; Chukwu et al. 2018). For this study, we follow the procedures of Okubo et al. (1985) and Tanaka et al. (1999).

From the assumptions that a model layer extends infinitely far in all horizontal directions, depth to top bound of a magnetic source is small compared with the horizontal scale of a magnetic source, and magnetization $M(x, y)$ is a random function of x and y, the power density spectra of total field anomaly $\Phi_{\Delta T}$ (Tanaka et al. 1999):

$$\Phi_{\Delta T}\left(k_x, k_y\right) = \Phi_M\left(k_x, k_y\right) \times F\left(k_x, k_y\right),$$

$$F\left(k_x, k_y\right) = 4\pi^2 C_{\mathrm{m}}^2 |\Theta_{\mathrm{m}}|^2 |\Theta_{\mathrm{f}}|^2 \mathrm{e}^{-2|k|z_t}\left(1 - \mathrm{e}^{-|k|(z_{\mathrm{b}} - z_{\mathrm{t}})}\right)^2 \tag{1}$$

where Φ_M is power-density spectra of the magnetization, C_{m} is a proportionality constant, and Θ_{m} and Θ_{f} are factors for magnetization direction and geomagnetic field direction respectively. This equation can be simplified by noting that all terms, except $|\Theta_{\mathrm{m}}|^2$ and $|\Theta_{\mathrm{f}}|^2$, are radially symmetric. Moreover, the radial averages of Θ_{m} and Θ_{f} are constant. If $M(x, y)$ is completely random and uncorrelated, $\Phi_M\left(k_x, k_y\right)$ is a constant. Hence, the radial average of $\Phi_{\Delta T}$ is:

$$\Phi_{\Delta T}\left(|k|\right) = A\mathrm{e}^{-2|k|z_{\mathrm{t}}}\left(1 - \mathrm{e}^{-|k|(z_{\mathrm{b}} - z_{\mathrm{t}})}\right)^2 \tag{2}$$

where A is a constant. For wavelengths less than about twice the thickness of the layer, Eq. 2 approximately becomes:

$$\ln\left[\Phi_{\Delta T}\left(|k|\right)^{1/2}\right] = \ln B - |k|\, z_{\mathrm{t}} \tag{3}$$

where B is a constant. Using the slope of the power spectrum, one could estimate the top bound of a magnetic source. On the other hand, Eq. 2 rewrites as:

$$\Phi_{\Delta T}(|k|)^{1/2} = C\mathrm{e}^{-|k|z_{\mathrm{o}}}\left(\mathrm{e}^{-|k|(z_{\mathrm{t}} - z_{\mathrm{o}})} - \mathrm{e}^{-|k|(z_{\mathrm{b}} - z_{\mathrm{o}})}\right) \tag{4}$$

where C is a constant. At long wavelengths, Eq. 4 is:

$$\Phi_{\Delta T}(|k|)^{1/2} = C\mathrm{e}^{-|k|z_{\mathrm{o}}}\left(\mathrm{e}^{-|k|(-d)} - \mathrm{e}^{-|k|(-d)}\right) \sim C\mathrm{e}^{-|k|z_{\mathrm{o}}} 2\,|k|\,d \tag{5}$$

where $2d$ is the thickness of the magnetic source. From Eq. 5

$$\ln\left\{\left[\Phi_{\Delta T}\left(|k|\right)^{1/2} / \,|k|\right]\right\} = \ln D - |k|\, z_{\mathrm{o}} \tag{6}$$

where D is a constant. We summarize Eqs. (3) and (6) as

$$\ln\left[P(k)^{1/2}\right] = \ln B - |k|\, z_{\mathrm{t}} \tag{7}$$

and,

$$\ln\left[P(k)^{1/2}/\,|k|\right] = \ln D - |k|\, z_{\mathrm{o}} \tag{8}$$

where $\Phi_{\Delta T}(|k|)^{1/2}$ is written as $P(k)^{1/2}$.

We estimated the top bound and the centroid of the magnetic source by fitting a straight line through the high wavenumber and low-wavenumber parts of the radially average spectrum of $\ln\left[P(k)^{1/2}\right]$ and $\ln\left[P(k)^{1/2}/\,|k|\right]$ from Eqs. (7) and (8) respectively. As our frequency unit is in cycles per kilometer, we divided the corresponding spectrum relation by (4π). The depth to bottom (basal depth) of the magnetic source is given by;

$$z_{\mathrm{b}} = 2z_{\mathrm{o}} - z_{\mathrm{t}} \tag{9}$$

CPD is assumed as the obtained basal depth computations (Okubo et al. 1985; Tanaka et al. 1999).

Conductive Heat Flow

Fundamental relation when considering conductive heat conveyance is Fourier's law (Tanaka et al. 1999). In the one-dimensional case, assuming a vertical direction for temperature variation and constant temperature gradient dT/dz, Fourier's law takes the form

$$\mathrm{q} = \mathrm{k}\frac{\mathrm{dT}}{\mathrm{dz}} \tag{10}$$

where q is describe as the heat flux, k, the coefficient of thermal conductivity.

The Curie temperature (θ) can be defined:

$$\theta = \left(\frac{\mathrm{dT}}{\mathrm{dz}}\right)\mathrm{z}_{\mathrm{b}} \tag{11}$$

where z_{b} is the Curie point depth, provided that there is no heat sources or heat sinks between the earth's surface and the Curie point depth, the surface temperature is 0 ºC, and dT/dz is constant. We utilize the Curie point (θ) for magnetite (580 °C with an average thermal conductivity of 1.80 $\mathrm{Wm}^{-1}\,\mathrm{k}^{-1}$ for the sedimentary formation and 2.5 $\mathrm{Wm}^{-1}\,\mathrm{k}^{-1}$ (Manea and Manea 2011) for the region with igneous rock.

The aeromagnetic data utilized in this research was collected by the Nigeria Geological Survey Agency (NGSA) during the period from 2005 to 2009. The data was gathered with an average terrain clearance of 80 m and 500 m line spacing. The geomagnetic gradient was removed from the aeromagnetic data using the 2005 International Geomagnetic Reference Field (IGRF) formula. We used data reduced to the equator (RTE) in our analysis of the magnetic data. Leu demonstrated that the RTE technique was more reliable at high latitudes than the Reduction to Pole (RTP) technique is at low latitudes. Jain (1988) compared the RTP with RTE techniques and concluded that the RTE technique is preferable, more particularly at the middle and lower latitudes. In our study area located at lower latitudes, we utilized the fast Fourier transform operator to apply the RTE correction, assuming a magnetic declination of -2.15° and an inclination of -13.91°. To remove the effects of topography on the aeromagnetic anomalies, the RTE data were low-pass-filtered and the resulting map displayed in Fig. 4.

In selecting our block size, an effort was made to follow the suggestion by Ravat et al. (2007) to consider information on spectrum depth to instruct on window lengths chosen. The depth resolution is constrained by the length of the aeromagnetic profile (L), and the maximum estimation of CPD is restricted to (L)/2π (Shuey et al. 1977; Manea and Manea 2011). If the bases of the source bodies are deeper than L/2π, the spectral analysis procedure may not be feasible (Salem et al. 2000). To address this, we partitioned the magnetic anomaly map into subregions measuring 110 × 110 km, with the blocks overlapping by 50% of the block size. An additional block was sampled by placing center point of the subregions within the central part of the study area following Ross et al. (2006). A total of 5 adequately overlapped blocks were obtained at 110 × 110 km dimension. The statistical errors for each of the selected windows were computed from the standard deviation of differences between the natural logarithm of power density spectrum and the linear fit from the least square method. The range of frequencies considered for these evaluations were taken within the range of the linear fits on each spectrum. This technique has been successfully applied by Manea and Manea (2011), Trifonova et al. (2009) and Okubo and Matsunaga (1994). Figure 5 shows an example of the radially averaged power spectrum plot for block 1. The centroid depth and its computed uncertainty stood at 7.27 ± 0.05 km and depth to the top (DTT) of magnetic source, 0.89 ± 0.02 km, CPD for block 1 was calculated as 13.66 ± 0.48 km.

Results

A map display of the estimated DTT is shown in Fig. 6 and the basal depths (CPDs) is displayed in Fig. 7. Figure 8 display a 3D plot of the DTT and CPD for the RZHS region. The computed heat flow is displayed in Fig. 9.

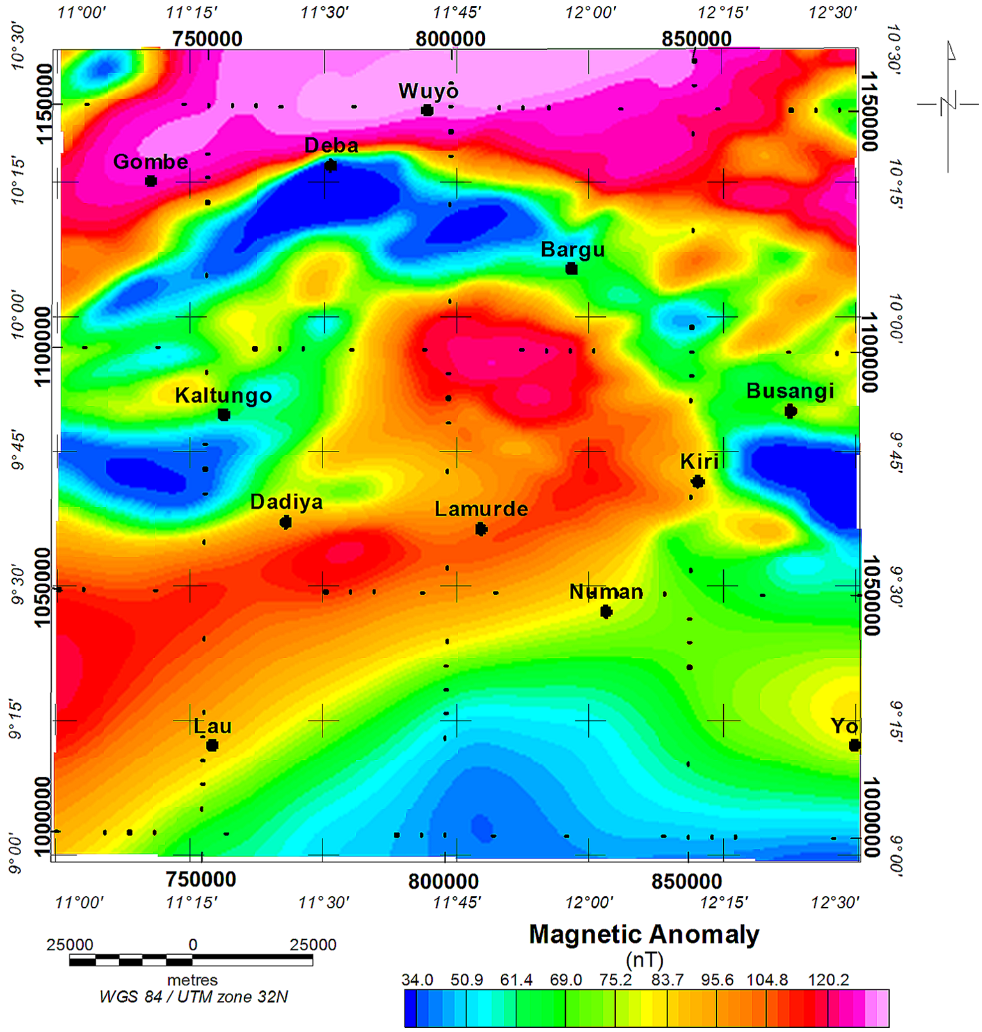

Fig. 4 Magnetic anomaly map of the study area. High and low values of the magnetic field could be seen in the study area, with the magnetic highs notable in the central and northern regions of the area. Both the high and low magnetic anomalies are distributed within the sedimentary and basement terrains of the region

Discussion

The relationship between topography and heat flow in a region is primarily influenced by the geological characteristics of the area. A comparison of the regional topography (Fig. 2) with the geological map (Fig. 3) show a striking surficial semblance with most of the features traced on the topographic map given interpretation on the geological map. At the location of RZHS (Lamurde), a complicated interplay of geology is seen between the sedimentary formation and crystalline basement. This region clearly show the aftermath of a serious tectonic event that ensured at the region. We believe that the tectonic activities that occurred at the region is instrumental to the formation of the RZHS. Regions with active tectonics experience higher heat flow due to the movement of tectonic plates and associated geological process. The tectonic deformation at this region has been described by Haruna et al. (2012) to have superimposed the Pan-African mylonitic shear zones, providing post depositional fractures and fault zones. These geological features impacted the distribution of thermal anomalies in the region.

Analysis of Fig. 4 reveal distinct magnetic anomalies in the RZHS region, indicative of subsurface geological structures associated with potential geothermal reservoirs. The distinctive spatial distribution of magnetic anomalies at the Lamurde location coupled with the complicated geology, suggests the presence of fault systems and other features which are favorable indicators for geothermal energy exploration.

The DTT ranges between 0.89 and 1.08 km. Lamurde region locates directly over the Bima Sandstone whose depths have earlier been estimated at between 0.4 and 0.9 km (Umeji 2013). This depths is in agreement with our estimated DTT of magnetic sources for the location. A plot of DTT (Fig. 6) show an average of 1.0 km at the RZHS location and becomes deeper northwards. Results from the CPD evaluations (Table 1) show values ranging between 9.96 ± 0.21 and ± 1.10 km with their corresponding uncertainties. An average value of 12.11 km was realized for the

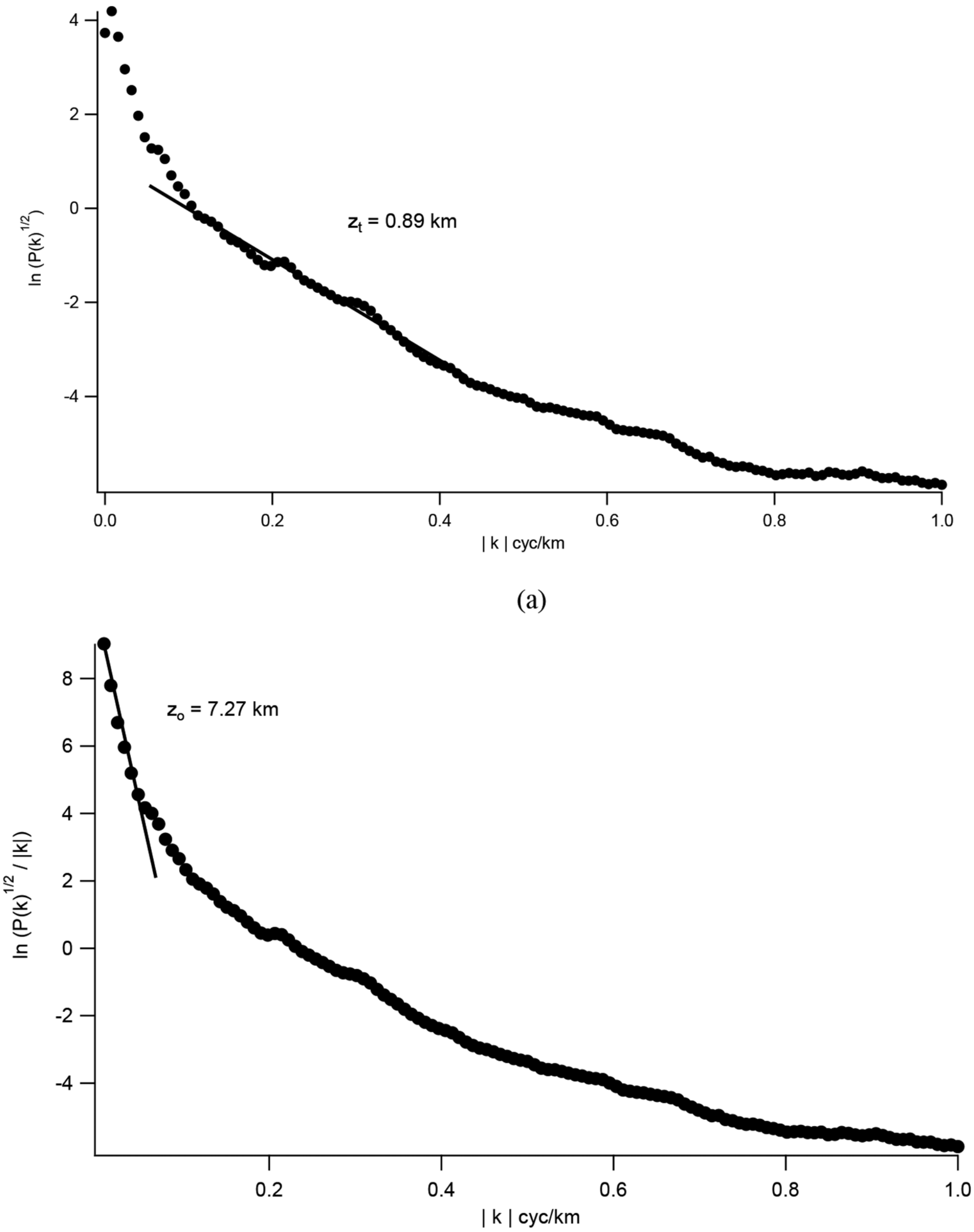

(b)

Fig. 5 Radially averaged power spectrum plot for block 1. (a) depth to the top (DTT) (z_t) computed for this block show an average value of 0.89 km. (b) depth to the centroid (z_o) computed for this block show an average value of 7.27 km

Table 1 Results of spectral analysis and depth estimations of magnetic sources including error estimations for the selected blocks

Blocks	Longitudes (°)	Latitudes (°)	z_t (km)	Error (±km) z_t	z_o (km)	Error (±km) z_o	z_b (km)	Error (±km) z_b
1	11.50	9.50	0.89	0.02	7.27	0.05	13.66	0.48
2	12.00	9.50	0.97	0.01	5.70	0.13	10.43	0.62
3	12.00	10.00	1.05	0.01	6.30	0.04	11.56	0.25
4	11.50	10.00	1.01	0.03	7.97	0.18	14.92	1.10
5	11.75	9.75	1.08	0.01	5.52	0.05	9.96	0.21

coverage area. A plot of this values (Fig. 7) reveal an average CPD value of 10.5 km at the RZHS location. This value indicates shallow CPDs in the region compared with other parts of the study area, as the CPD increases away from the Lamurde region. Tanaka et al. (1999) noted that the CPDs are relatively shallow, with depths of approximately 10 km in volcanic and geothermal areas, 15 to 25 km in island arcs and ridges, over 20 km in plateaus, and exceeding 30 km

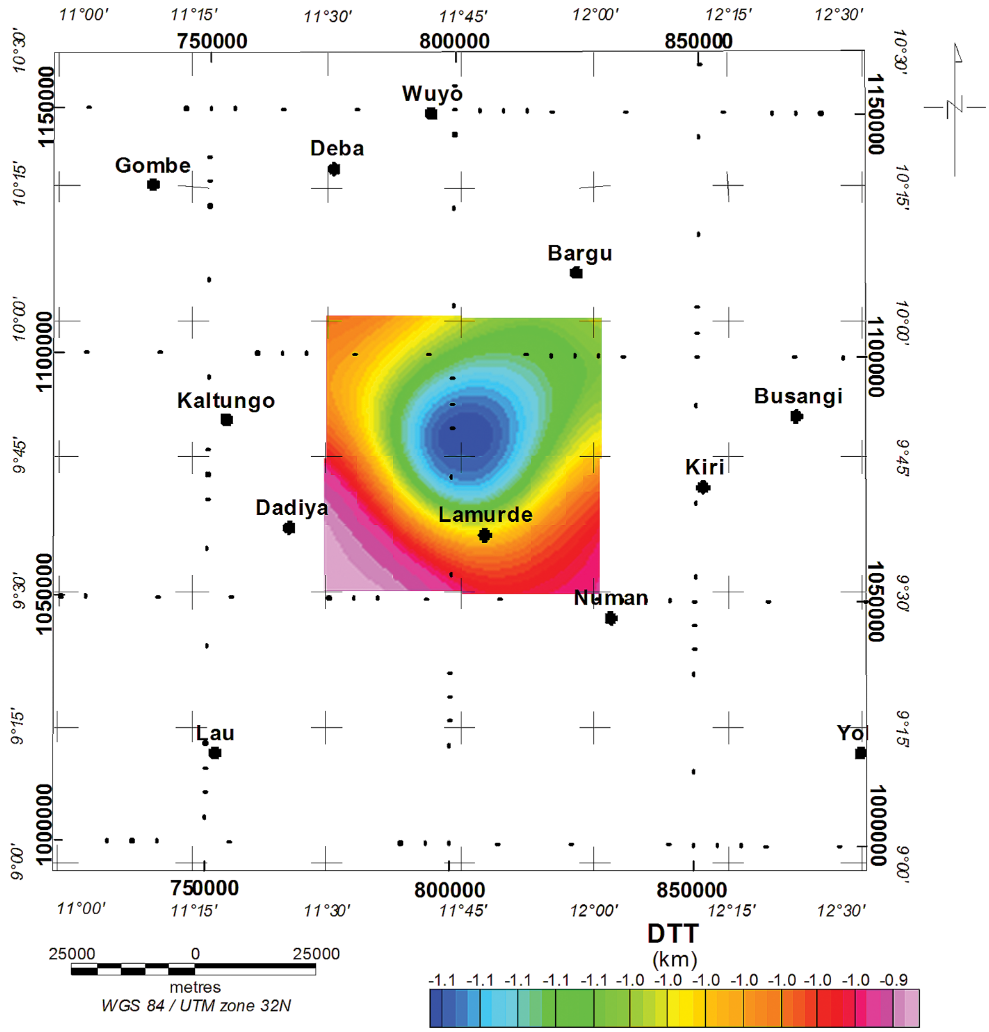

Fig. 6 Depth to the top (DTT) of magnetic source z_t

in trenches. The presence of RZHS in the study area aligns with the characteristics described for the first category. We believe that the shallow CPD at this location could be responsible for the surficial heat signatures seen in the RZHS. RZHS locates at the foot of the Lamurde anticline that stretches southwards. We believe that the upliftment of the anticline and magmatic structure that intruded the area; conducts heat from the magma to heat the reservoir rock above it. This process also provides the heat acquired by the RZHS reservoir within the subsurface.

An opposite orientation is observed from the 3D plots of DTT and CPD (Fig. 8) with regions of deeper DTT corresponding to shallow CPD and vice versa. It becomes clearer that the Lamurde area sits atop a protruded magmatic intrusion in the subsurface which is equally complimented by a thin top layer at the location. We propose that the heat source for the RZHS could have possibly originated from an intrusion with possible connection to the magma chamber at depth. This may have resulted in the exposure of rock units in the area to direct heating from the Earth's mantle. The basement complex of Nigeria is occasionally intruded and interspersed by older granites that originated during the Pan-African orogeny. This inference is further substantiated by the intricate geology of the region.

The minimum heat flow value required for considerable generation of geothermal energy is approximately $60\mathrm{mWm}^{-2}$ (Jessop et al., 1975). Estimated heat flow values at the location varies between 76.62 and 138.29 mWm^{-2} with an average of 91.66 mWm^{-2} (Fig. 9). With values reaching as high as 138 mWm^{-2} in the region, we propose an anomalous subsurface geothermal condition which could be further investigated.

Conclusion

The assessment of geothermal energy potential in the Ruwan-Zafi Hot Spring (RZHS) region, northeastern Nigeria, utilizing high-resolution aeromagnetic data has revealed promising indications of subsurface geological structures

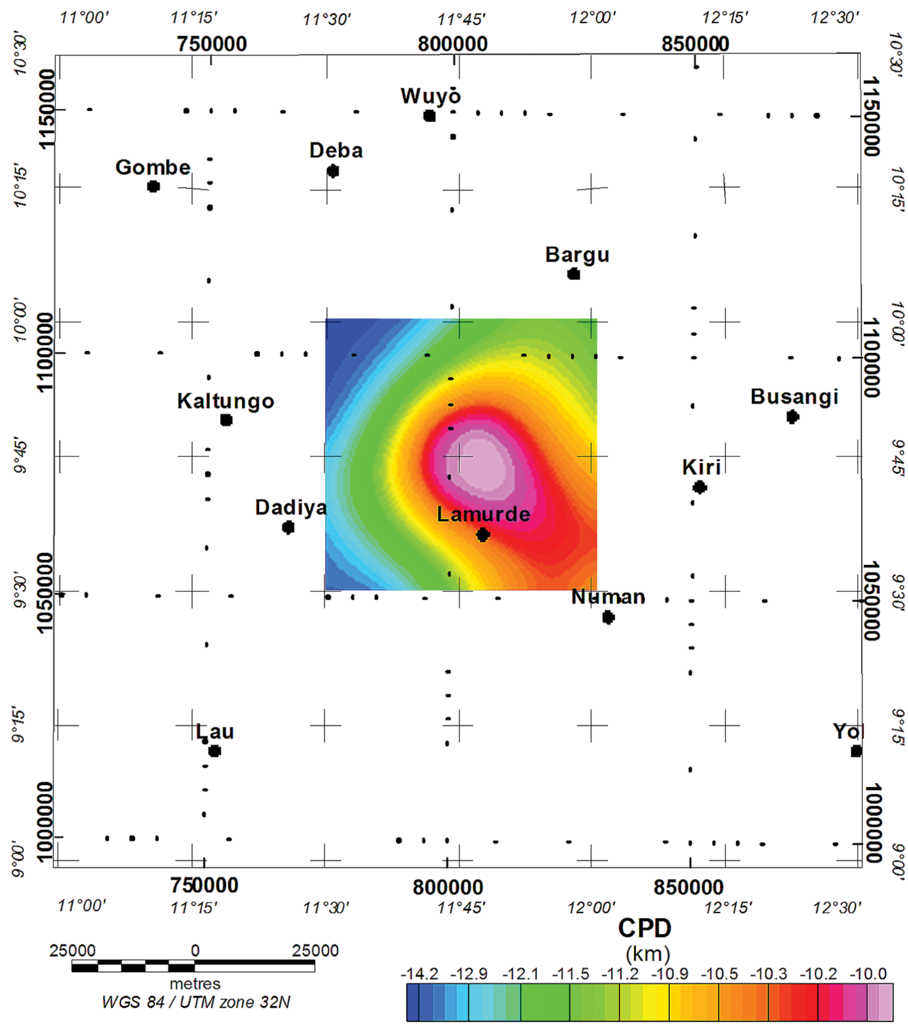

Fig. 7 Estimated CPD for the study area

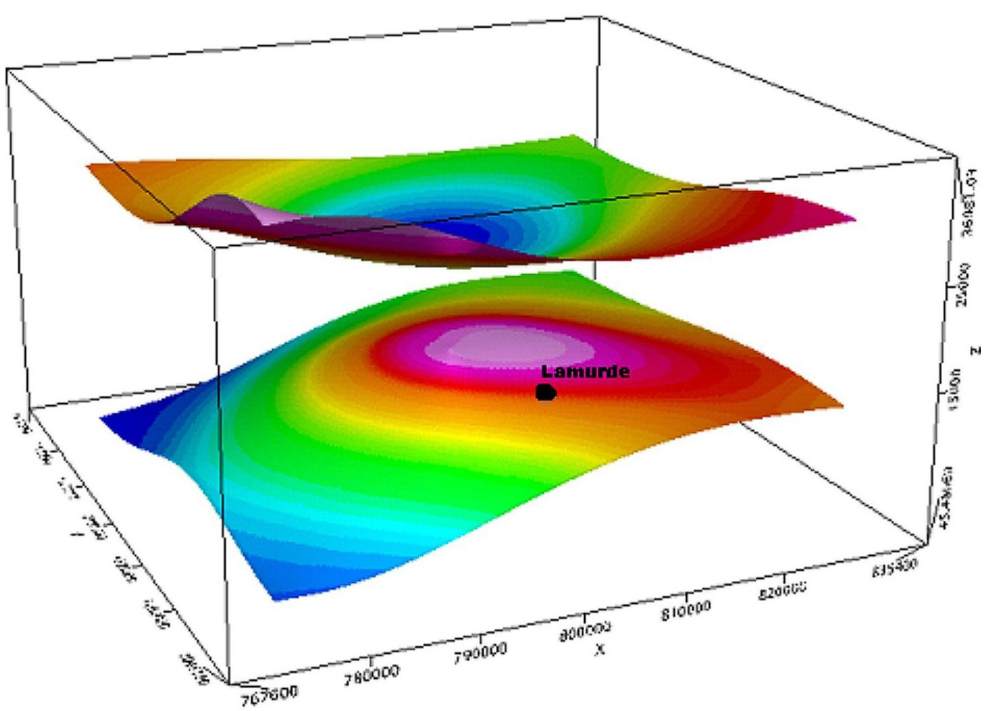

Fig. 8 3D plot of DTT and CPD of the RZHS region

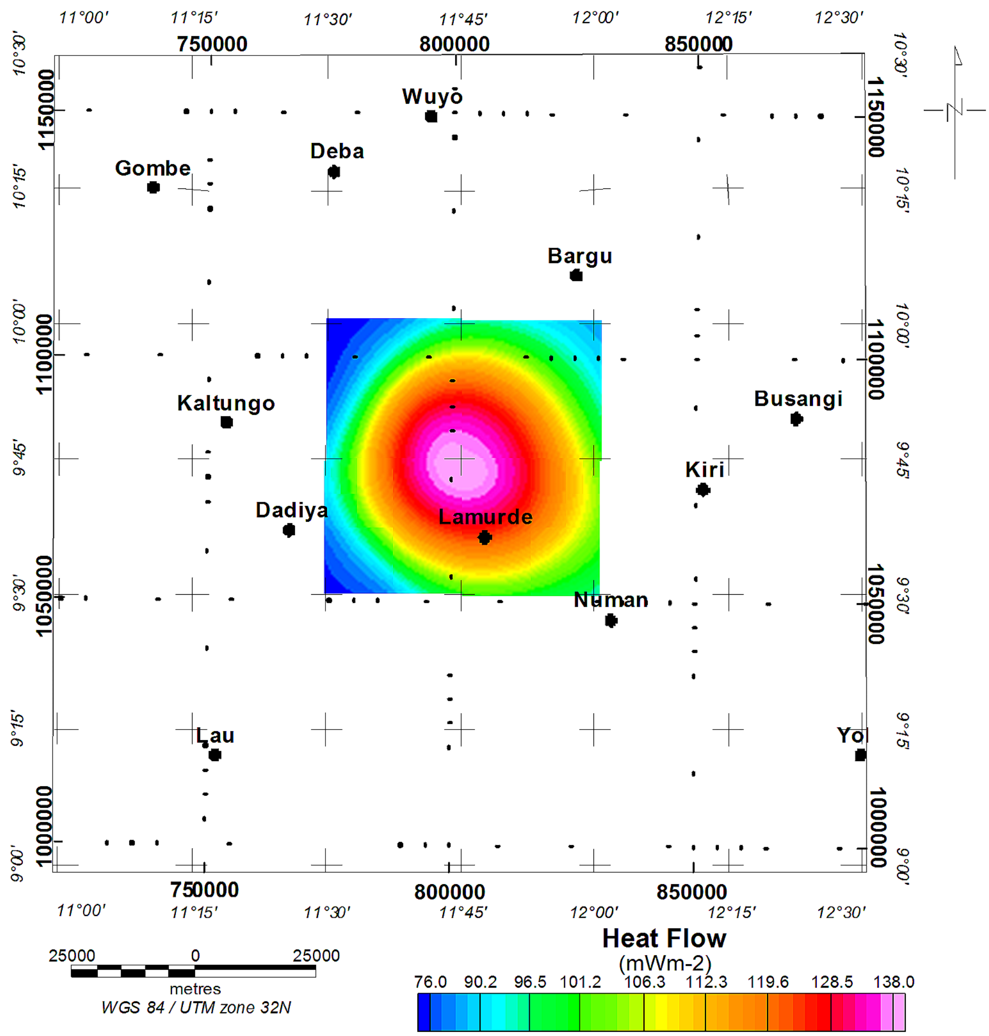

Fig. 9 Heat flow map of the RZHS region derived from the CPD computations

conducive to geothermal resource development. The data was analyzed using the spectral method to estimate CPD and crustal heat flow at RZHS. The result reveals CPDs varying between 9.96 and 14.92 km. Estimated crustal heat flow varies between 72.62 and 138.29 mWm^{-2} with a value of 128.5 mWm^{-2} at the RZHS location. The shallow CPDs in at the RZHS location indicates the viability of the area for further geothermal energy investigation. The presence of fault systems and subsurface intrusions in the location also suggests a geologically favorable environment for the development and exploitation of geothermal resources. This study would also contribute to the diversification of Nigeria's energy mix by the addition of geothermal energy resources.

Data availability The data utilized in this study is accessible upon request from the corresponding author.

Declarations

Conflict of interest On behalf of all authors, the corresponding author states that there is no conflict of interest.

References

Abraham E, Itumoh O, Chukwu C, Rock O (2018) Pure appl Geophys 176:22–36. https://doi.org/10.1007/s00024-018-2028-1. Geothermal Energy Reconnaissance of Southeastern Nigeria from Analysis of Aeromagnetic and Gravity Data

Adepelumi AA, Olorunfemi MO (2019) Geothermal energy potentials of Nigeria: a review. J Earth Sci Geotech Eng 9(4):101–116

Akintude AO, Oladele S, Ojo AA (2017) Integration of remote sensing and geophysical data for geothermal potential assessment in Northeastern Nigeria. Renewable Energy 107:330–340

Al-Ghriybah M, Alnsour MA, Al-Hyari L (2023) Using Weibull distribution model for wind energy analysis of small-scale power generation at Al-Salt city in Jordan. Model Earth Syst Environ 9:2651–2661. https://doi.org/10.1007/s40808-022-01643-9

Anakwuba E, Okeke H, Chinwuko I, Onyekwelu C (2016) Estimation of Curie isotherm and heat flow of eastern Chad basin, Nigeria from spectral analysis of aeromagnetic data. SEG, International Conference and Exhibition, Barcelona, Spain, 3–6 April 2016

Bansal AR, Anand SP, Rajaram M, Rao VK, Dimri VP (2013) Depth to the bottom of magnetic sources (DBMS) from aeromagnetic data of Central India using modified centroid method for fractal distribution of sources. Tectonophysics 603:155–161

Bazilian M, Hobbs B, Blyth W, MacGill I, Howells M, Arent N (2011) Considering the energy, water and food nexus: towards an integrated modelling approach. Renew Sustain Energy Rev 15(9):5896–5903

Benkhelil J (1982) Benue Trough and Benue Chain. Geol Mag 119:115–168

Benkhelil J (1986) Structure et évolution geodynamique du basin intercontinental de la Bénoué (Nigeria). Thése de Doctorat d'Etat, Université de Nice. P. 226

Benkhelil J, Robineau B (1983) Le Fosse de la Benoue est-Il Un rift? Bull. Centres Recherches Expl Prod Elf-Aquitaine 7:315–321

Bhattacharyya BK, Leu LK (1975) Spectral analysis of gravity and magnetic anomalies due to two-dimensional structures. Geophysics 40:993–1013

Blakely RJ (1988) Curie temperature analysis and tectonic implications of aeromagnetic data from Nevada. J Geophy Res: Solid Earth 93:11817–11832

Chukwu CG, Udensi EE, Abraham EM, Ekwe AC, Selemo AO (2018) Geothermal energy potential from analysis of aeromagnetic data of part of the Niger-Delta Basin, Southern Nigeria. Energy 143:846–853. https://doi.org/10.1016/j.energy.2017.11.040

Dar FA, Venkateshwarlu M, Khan I et al (2024) Modeling the environment and climatic conditions of Ladakh Himalaya using Quaternary sediments. Model Earth Syst Environ. https://doi.org/10.1007/s40808-024-01965-w

Dolmaz MN, Ustaomer T, Hisarli ZM, Orbay N (2005) Curie point depth variations to infer thermal structure of the crust at the african-eurasian convergence zone, SW Turkey. Earth Planet Space 57:373–383

Eletta BE, Udensi EE (2012) Investigation of the Curie point isotherm from the magnetic fields of eastern sector of central Nigeria. Geosciences 2:101–106

Emetere ME, Akpan GE (2022) Investigation of potential geothermal well locations in Nigeria using remote sensing and field measurement. Int J Sus Energy 42:1. https://doi.org/10.1080/14786451.2023.2217950

Grogan L (2015) Energy access and forest dependence: evidence from rural Liberia. J Dev Econ 118:68–79

Guiraud M (1990) Tectono-sedimentary framework of the early cretaceous continental bima formation (Upper Benue Trough, Northeastern Nigeria). J Afr Earth Sci 10:341–353

Guiraud M, Maurin JC (1992) Early cretaceous rifts of Western and Central Africa: an overview. Tectono-phys 213:153–168

Haruna IV, Ahmed HA, AS (2012) Geology and tectono-sedimentary disposition of the Bima sandstone of the Upper Benue Trough (Nigeria): implications for sandstone-hosted uranium deposits. J Geol Min Res 4(7):168–173

Ijeh BI, Anyadiegwu FC, Onwubuariri CN et al (2023) Evaluation of geothermal resource potential of the Lower Benue Trough using aeromagnetic and radiometric data. Model Earth Syst Environ 10:695–721. https://doi.org/10.1007/s40808-023-01796-1

Ishola KS, Akerele PO, Folarin O et al (2020) Application of aeromagnetic data to map subsurface structural features in Ewekoro, Southwestern Nigeria. Model Earth Syst Environ 6:2291–2302. https://doi.org/10.1007/s40808-020-00812-y

Jain S (1988) Total magnetic field reduction—the Pole or Equator? A model study. Can J Explor Geophys 24(2):185–192

Jessop AM, Habart MA, Sclater JG (1975) The world heat flow data collection. Geotherm Serv Can Geotherm Ser 50:55–77

Kammen DM, Agusdinata DB (1997) A rural energy model for Indonesia. Energy Sustain Dev 4(2):31–36

Kassem Y, Gökçekuş H, Iravanian A, Gökçekuş R (2022) Predictive suitability of renewable energy for desalination plants: the case of güzelyurt region in northern Cyprus. Model Earth Syst Environ 8:3657–3677. https://doi.org/10.1007/s40808-021-01315-0

Khandker SR, Barnes DF, Samad HA (2009) Energy Poverty in Rural Bangladesh. World Bank

Maden N (2009) Crustal thermal properties of the Central Pontides (Northern Turkey) deduced from spectral analysis of magnetic data. Turkish J Earth Sci 18:1–10

Manea M, Manea VC (2011) Curie point depth estimates and correlation with subduction in Mexico. Pure Appl Geophy 168:1489. https://doi.org/10.1007/s00024-010-0238-2

Maurin JC, Benkhelil J, Robineau B (1985) Fault rocks of the Kaltungo Lineament (northeastern Nigeria) and their relationship with the Benue Trough. J Geol Soc Lond 143:587–599

Mayhew MA (1985) Curie isotherm surfaces inferred from high altitude magnetic anomaly data. J Geophys Res: Solid Earth 90(B3):2647–2654

Obande GE, Lawal KM, Ahmed LA (2014) Spectral analysis of aeromagnetic data for geothermal investigation of Wikki warm spring, north-east Nigeria. Geothermics 50:85–90

Ojoawo AI, Sedara S (2016) Magnetic data analysis for potential geothermal energy development: case of Ikogosi warm spring, Ekiti, Southwestern Nigeria. Elixir Earth Sci 100:43660–43664

Okubo Y, Matsunaga T (1994) Curie point depth in northeast Japan and its correlation with regional thermal structure and seismicity. J Geophys Res: Solid Earth 99:22363–22371

Okubo Y, Graf RJ, Hansen RO, Ogawa K, Tsu H (1985) Curie point depths of the island of Kyushu and surrounding areas, Japan. Geophysics 53(3):481–494

Okubo Y, Matsushima J, Correia A (2003) Magnetic spectral analysis in Portugal and its adjacent seas. Phys Chem Earth 28:511–519

Onyejiuwaka IS, Iduma UK (2020) Assessment of Geothermal Energy Potential of Ruwan Zafi, Adamawa State and environs, northeastern Nigeria, using high Resolution Airborne magnetic data. Cur Res Geosc 10(115). https://doi.org/10.3844/ajgsp.2020.1.15

Oyedepo SO (2012) Energy and sustainable development in Nigeria: the way forward. Energy Sustain Soc 2:15

Rabeh TT, El Rahman AAA (2022) Illustrating the active faults using integrated geophysical data along the Suez Canal-district, Eastern Desert, Egypt. Model Earth Syst Environ 8:5053–5059. https://doi.org/10.1007/s40808-022-01382-x

Rajaram M, Anand SP, Hemant K, Purucker ME (2009) Curie isotherm map of Indian subcontinent from satellite and aeromagnetic data. Earth Planet Sci Lett 281:147–158

Ravat D, Pignatelli A, Nicolosi I, Chiappini M (2007) A study of spectral methods of estimating the depth to the bottom of magnetic sources from near-surface magnetic anomaly data. Geophys J Int 169:421–434

Ross HE, Blakely RJ, Zoback MD (2006) Testing the use of aeromagnetic data for the determination of Curie depth in California. Geophysics 71(5):L51–L59

Salem A, Ushijima K, Elsiraft A, Mizunaga H (2000) Spectral analysis of aeromagnetic data for geothermal reconnaissance of Quseir area, northern Red Sea, Egypt. Proceedings of the world geothermal congress: 1669–1674

Selvarajoo A, Muhammad D, Arumugasamy SK (2020) An experimental and modelling approach to produce biochar from banana peels through pyrolysis as potential renewable energy resources. Model Earth Syst Environ 6:115–128. https://doi.org/10.1007/s40808-019-00663-2

Shuey RT, Schellinger DK, Tripp AC, Alley LB (1977) Curie depth determination from aeromagnetic spectra. Geophy J Inter 50:75–101

Sovacool BK, Dworkin MH (2015) Energy justice: conceptual insights and practical applications. Energy Policy 105:658–667

Spector A, Grant FS (1970) Statistical models for interpreting aeromagnetic data. Geophysics 35:293–302
Stampolidis A, Tsokas G (2002) Curie point depths of Macedonia and Thrace, N. Greece. Pure appl Geophys 159:1–13
Tanaka A, Okubo Y, Matsubayashi O (1999) Curie-temperature isotherm depth based on spectrum analysis of the magnetic anomaly data in east and southwestern Asia. Tectonophysics 306:461–470
Trifonova P, Zheler Z, Petrova T (2006) Curie point depths of the Bulgarian territory inferred from geomagnetic observations. Bulgarian Geophy J 32:12–23
Trifonova P, Zheler Z, Petrova T, Bojadgieva K (2009) Curie point depths of the Bulgarian territory inferred from geomagnetic observations and its correlation with regional thermal structure and seismicity. Tectonophysics 473:362–374
Tsokas G, Hansen RO, Fyticas M (1998) Curie point depth of the island of Crete (Greece). Pure Appl Geophy 159:1–13
Umeji O (2013) The south and central Benue trough: stratigraphic revisions. In book: Proceedings of University of Jos PTDF Chair Endowment Fund Seminar, April 2012Edition: First 2013 Chapter: No. 4 Publisher: University of Jos, PTDF EMC
Yakubu JA, Okeke FN, Obiora DN (2020) Estimation of Curie point depth, geothermal gradient and heat flow within the lower Benue trough, Nigeria using high resolution aeromagnetic data. Model Earth Syst Environ 6:1439–1449. https://doi.org/10.1007/s40808-020-00760-7

Publisher's Note Springer Nature remains neutral with regard to jurisdictional claims in published maps and institutional affiliations.